



PCCP

Aromatic Character of [Au₁₃]⁵⁺ and [MAu₁₂]^{4+/6+} (M=Pd,Pt) Core in Ligand Protected Gold Nanoclusters. Interplay Between Spherical and Planar σ -Aromatics

Journal:	<i>Physical Chemistry Chemical Physics</i>
Manuscript ID	CP-ART-08-2019-004477.R1
Article Type:	Paper
Date Submitted by the Author:	01-Oct-2019
Complete List of Authors:	Fedik, Nikita; Utah State University, Chemistry and Biochemistry Boldyrev, Alexander; Utah State University, Department of Chemistry and Biochemistry Muñoz-Castro, Alvaro; Universidad Autonoma de Chile,

SCHOLARONE™
Manuscripts

ARTICLE

Aromatic Character of $[\text{Au}_{13}]^{5+}$ and $[\text{MAu}_{12}]^{4+/6+}$ ($\text{M}=\text{Pd},\text{Pt}$) Core in Ligand Protected Gold Nanoclusters. Interplay Between Spherical and Planar σ -Aromatics

Received 00th January 20xx,
Accepted 00th January 20xx

DOI: 10.1039/x0xx00000x

Nikita Fedik,^a Alexander Boldyrev,^{*a} and Alvaro Muñoz-Castro^{*b}

The most characteristic feature for planar π -aromatics is the ability to sustain a long-range shielding cone under a magnetic field oriented in a specific direction. In this article we showed that similar magnetic responses can be found in σ -aromatic and spherical aromatic systems. For $[\text{Au}_{13}]^{5+}$ long-range characteristics of the induced magnetic field in the bare icosahedral core are revealed, which are also found in the ligand protected $[\text{Au}_{25}(\text{SH})_{18}]^{-}$ model, proving its spherical aromatic properties, also supported by the AdNDP analysis. Such properties are given by the 8-ve of the structural core satisfying the Hirsch $2(N+1)^2$ rule, which is also found in the isoelectronic $[\text{M@Au}_{12}]^{4+}$ core, a part of $[\text{MAu}_{24}(\text{SR})_{18}]^{2-}$ ($\text{M}=\text{Pd},\text{Pt}$) cluster. This contrasts to the $[\text{M@Au}_{12}]^{6+}$ core in $[\text{MAu}_{24}(\text{SR})_{18}]^0$ ($\text{M}=\text{Pd},\text{Pt}$), representing 6-ve superatoms, which exhibit characteristics for planar σ -aromatics. Our results support the spherical aromatic character of stable superatoms, whereas the 6-ve intermediate electron counts satisfy the $4N+2$ rule (applicable for both π - and σ -aromatics), showing the reversible and controlled interplay between 3D spherical and 2D σ -aromatic clusters.

Introduction

Since the early characterization of thiolate-protected gold nanoclusters,¹ considerable efforts have been paid driven by their potential role as efficient building blocks for functional nanomaterials.^{2–11} Currently synthetic methods are able to achieve atomically-precise clusters^{12,13}. It became possible to render relevant structures at nanosized domains (< 2 nm) to study the evolution from small aggregates to nanocrystals. Their molecule-like bandgap^{14–17} and novel properties are useful towards promising applications in catalysis, sensing, and biomedicine among others.^{10,11,18–24}

Amidst the different thiolate-protected gold clusters, $\text{Au}_{25}(\text{SR})_{18}$ is one of the most prominent member²⁵ displaying high stability against degradation. This remarkable stability originates from both geometric and electronic characteristics.^{6,26–29} Its structure is composed by a formally $[\text{Au}_{13}]^{5+}$ core unit with 8-valence electrons (ve),^{7,17} ensuring the occupancy of S and P superatomic electronic shells in its anionic $[\text{Au}_{25}(\text{SR})_{18}]^{-}$ form.^{30–32} Such electronic configuration resembles the one of noble gas atom and is responsible for their unprecedented stability. Further doping of Au_{25} with Pd and

Pt located at the endohedral site improves the cluster versatility resulting in $\text{M@Au}_{24}(\text{SR})_{18}$ species^{33,34} characterized in both dianionic and neutral charge states. This enables interconversion between 8- and 6-ve superatomic clusters.³⁵ Interestingly, the 8-ve count also fulfills the $2(N+1)^2$ Hirsch rule for spherical aromatic structures as an extension of the classical $(4N+2)$ Hückel rule.^{36,37} Hirsch rule^[36–39] recognizes three-dimensional molecules having pattern similar to classic two-dimensional aromatic species known for their remarkable stability.

However, the language that community uses to discuss spherically aromatic structures is not completely settled, and in the literature they are sometimes referred as superatoms (due to resemblance of their bond shapes to the atomic orbitals) or 3D aromatics as it was initially proposed by Lipscomb. To overcome any terminology discrepancies we would like to explicitly specify that all these terms are absolutely interchangeable and describe the same phenomenon^[40, 41].

Recently we have extended the approach of magnetic criteria of aromaticity providing another reliable method for studying spherical aromatic clusters based on their long-range magnetic behavior owing to the formation of a shielding cone in analogy to planar aromatics, as common property.⁴² Such approach is not influenced by the local response from each face in the spherical cage due to its focus on long-range behavior, which is more critical in heavy-elements.⁴³ Herein, we addressed a further understanding of stable gold clusters based on the $[\text{Au}_{13}]^{5+}$ considering their spherical aromatic features. Also we analyzed $[\text{M@Au}_{12}]^{4+}$ and $[\text{M@Au}_{12}]^{6+}$ cores observed in $[\text{MAu}_{24}(\text{SR})_{18}]^{2-}$ and

^a Department of Chemistry and Biochemistry, Utah State University, 0300, Old Main Hill, Logan, Utah, 84322-0300, USA E-mail: a.i.boldyrev@usu.edu

^b Grupo de Química Inorgánica y Materiales Moleculares, Facultad de Ingeniería, Universidad Autónoma de Chile, El Llano Subercaseaux 2801, Santiago, Chile.

† Footnotes relating to the title and/or authors should appear here.

Electronic Supplementary Information (ESI) available: [details of any supplementary information available should be included here]. See DOI: 10.1039/x0xx00000x

[MAu₂₄(SR)₁₈]⁰ (M=Pd and Pt) and showed that they could be denoted as 8- and 6-ve superatoms, respectively.

Computational Details

We deciphered their bonding patterns via Adaptive Natural Density Partitioning (AdNDP) analysis⁴⁴ which combines the concepts of localized and delocalized bonding crucial for solving complicated cases⁴⁵⁻⁴⁹. Magnetic response properties were also calculated to discuss aromatic character of clusters. Isosurfaces of the induced magnetic field were obtained as a three-dimensional grid of shielding tensor (σ_{ij}) given in ppm, with $B_i^{\text{ind}} = -\sigma_{ij}B_j^{\text{ext}}$ ⁵⁰⁻⁵⁴ depending on different representative orientations of the external field (B^{ext}) with the respect to i and j suffixes. They relate to the x -, y - and z -axes. These effects were considered within the GIAO formalism, employing the Perdew, Burke and Ernzerhof^{55,56} (OPBE-GGA) functional and triple- ξ Slater basis set plus the double-polarization (STO-TZ2P) basis set. Relativistic effects were taken into account via the ZORA Hamiltonian.⁵⁷ All calculations including structure optimization were performed using Relativistic DFT methods using the ADF 2016 code.⁵⁸ Relaxed structures were obtained at the TZ2P-PBE/ZORA level. Steps necessary to perform AdNDP analysis were carried out in Gaussian16⁵⁹ utilizing PBE0/def2-SVP level of theory⁶⁰.

Results and discussion

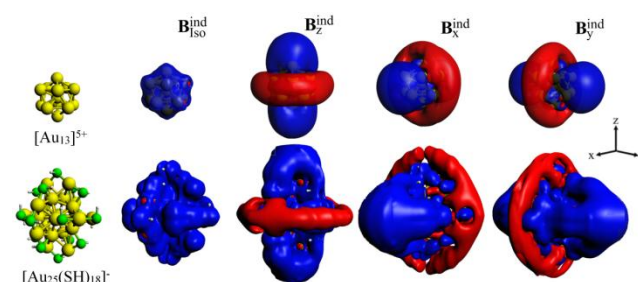
Spherical aromatic compounds have attracted a lot of attention and represent interesting extension to the concept of aromaticity, historically applied to π -planar organic structures. This relevant extension recognizes three-dimensional molecules which bonding pattern and stability resemble two-dimensional aromatic species.³⁶⁻³⁹ Among the studied thiolate-protected gold nanoparticles, [Au₂₅(SR)₁₈]⁻ is one of the most prominent example, providing a prototypical structure to evaluate properties of stable clusters. Its inner core is formally viewed as a [Au₁₃]⁵⁺ cluster (Figure 1) protected by a layer of organic ligands. The bare [Au₁₃]⁵⁺ cluster retains an icosahedral structure in contrast to the neutral counterpart, showing lower symmetry.⁶⁰⁻⁶⁴

The magnetic criteria of aromaticity^{54,65-67} have been well employed to evaluate spherical aromatic hollow cages,^{66,68} which is not straight in endohedral systems such as Au₁₃ and MAu₁₂ cores, where a central probe is highly influenced by the inner atom. To overcome such inconvenience, we focus on long-range characteristics of the induced magnetic field in bare [Au₁₃]⁵⁺, [Pd@Au₁₂]⁴⁺ and [Pd@Au₁₂]⁶⁺.

The isotropic response ($B_{\text{iso}}^{\text{ind}} = -(1/3)(\sigma_{xx} + \sigma_{yy} + \sigma_{zz})B^{\text{ext}}$) accounts for the orientational averaged behavior under a constant motion situation, such as in solution state (also denoted as NICS⁵⁹). In Figure 1, the obtained $B_{\text{iso}}^{\text{ind}}$ for [Au₁₃]⁵⁺ exhibits a continuous shielding region indicating the formation of currents. These currents generate a magnetic field that opposes the external field⁶⁹ (a 'diatropic' current) ruling the magnetic response of such cluster core. At distances of 8.5 Å from the center a shielding value of 3.0 ppm is observed. At

the inner section of the core shielding values higher to >-45.0 ppm are found, owing to the presence of the endohedral gold atom, whereas the hollow isoelectronic cage [Au₁₂]⁴⁺ depicts values of -35.0 ppm at the center. As has been shown for Hirsh aromatic fullerenes, the formation of shielding cone is parallel to the orientation of the applied field.⁴² Interestingly, such features remain in the overall ligand-protected [Au₂₅(SH)₁₈]⁻ cluster. These results support that the cluster-core features remain in the overall structure with a slight extension of the shielding cone owing to the contribution from the ligand-protecting layer (3 ppm ~10.0 Å). Thus, hereafter, we focus our effort in determining the magnetic response characteristics of MAu₁₂ cluster cores.

Figure 1. Magnetic response properties of [Au₁₃]⁵⁺ and



[Au₂₅(SH)₁₈]⁻, denoting the response under different orientations of the external field (B_z^{ind} , B_x^{ind} , and B_y^{ind}) and their isotropic (averaged) term ($B_{\text{iso}}^{\text{ind}}$). Isosurfaces set to ± 3 ppm, blue means shielding; red - deshielding.

To further confirm aromaticity the Adaptive Natural Density Partitioning (AdNDP) analysis was employed. The AdNDP analysis for [Au₁₃]⁵⁺ shows a set of four delocalized 13c-2e bonds in agreement to the 8-ve count fulfilling a $1S^21P^6$ electronic shell structure, satisfying the Hirsch rule for spherical aromatic compounds (Figure 2). This picture agrees with the molecular orbitals accounting for the superatomic 1S and 1P shells (Figure S1). The same holds when the ligand layer is taken into account in [Au₂₅(SH)₁₈]⁻, where the related set of four 13c-2e delocalized bonds supports the extension of the spherical aromatic properties from the bare core to the overall ligand-protected architecture. In addition, five localized lone pairs on every gold atom were located because of the complete occupancy of the $5d^{10}$ -Au shell (Figures S2). The aromatic character of the [Au₁₃]⁵⁺ cluster core is originated from the favorable $1S^21P^6$ electronic configuration, unraveling that the enhanced stability observed for [Au₂₅(SR)₁₈]⁻ clusters involves an aromatic behavior.

Further inclusion of dopant atoms is shown to increase the versatility of such species, resulting in more tailorable clusters.^{33,34} For the 8-ve monodoped cores [M@Au₁₂]⁴⁺, it is found that they are able to sustain the formation of shielding cone upon an external field at different orientations (Figure 3), which averages together to a continuous shielding region. Such features resemble the behavior found in [Au₁₃]⁵⁺ supported by the formation of shielding cone characteristics in several orientations owing to its inherent three-dimensional aromatic

properties as was observed for spherical aromatic fullerenes⁷⁰⁻⁷². Obviously, these properties are extensive to the related ligand-protected $[\text{MAu}_{24}(\text{SR})_{18}]^{2-}$ containing $[\text{M@Au}_{12}]^{4+}$ core. The AdNDP analysis shows a consequent set of four delocalized 13c-2e bonds satisfying the Hirsch rule meaning the similar bonding pattern between isoelectronic $[\text{M@Au}_{12}]^{4+}$ and $[\text{Au}_{13}]^{5+}$ cores enabling the spherical aromatic character (Figure 4, Figures S3, S5). Moreover, the icosahedral structure of $[\text{Au}_{13}]^{5+}$ core is preferred by the here discussed spherical aromatic characteristics.

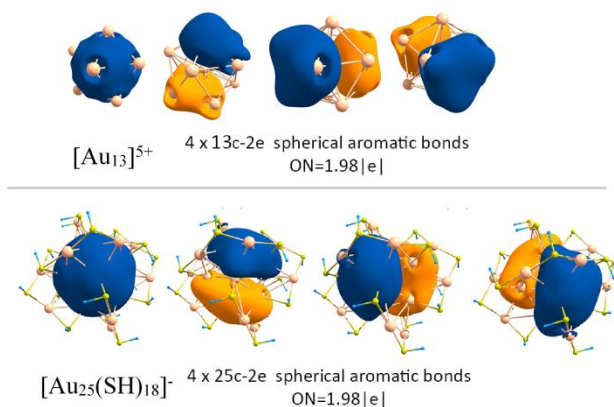


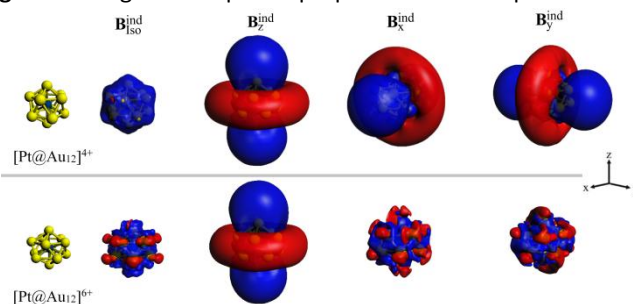
Figure 2. Chemical bonding pattern for $[\text{Au}_{13}]^{5+}$ and $[\text{Au}_{25}(\text{SH})_{18}]^{7-}$, as shown by the AdNDP analysis. ON stands for occupation number.

Noteworthy, reversible interconversion between neutral and dianionic species have been shown for $\text{MAu}_{24}(\text{SR})_{18}$ clusters, as proven by cyclic voltammetry among other experiments.³⁵ This opens a way to control a 6-ve \leftrightarrow 8-ve variation of its electronic structure in both monopalladium and monoplatinum structures. As a consequence, the nearly spherical icosahedral 8-ve MAu_{12} core is distorted leading to a flattened cage in its 6-ve form³⁵. In turn, it splits the parent $1\text{S}^21\text{P}^6$ shell after the removal of two electrons in $1\text{S}^21\text{P}_{x,y}^4$ and 1P_z^0 denoted as HOMO and LUMO respectively in the $[\text{MAu}_{12}]^{6+}$ core.

For such 6-ve species is interesting to evaluate if the aromatic properties are preserved or not, when the electron count deviates from the expected by the $2(\text{N}+1)^2$ Hirsch rule. Is it possible to find any resemblance of spherical aromatics despite of the unfavorable electron count? Indeed, AdNDP analysis for $[\text{MAu}_{12}]^{6+}$ shows now only three-sets of 13c-2e delocalized bonds (Figure 4, Figures S4, S6), accounting for its $1\text{S}^21\text{P}_{x,y}^4$ superatomic 2D-shell structure involving all the bare core atoms. It denotes a non-spherical aromatic character in this three dimensional structure. Alternatively we also localized the density only on Au_{10} ribbon and got set of three bonds having proper symmetry (Figure S7) but unreasonably low ONs in range 1.15-0.54|e|. We believe these results fully confirm that in order to construct delocalized bonds and bear aromatic properties (either 2D or 3D) contributions from all atoms are essential.

However, the experimentally demonstrated preference of neutral charge state of $[\text{MAu}_{24}(\text{SR})_{18}]^0$ clusters bearing 6-ve cluster cores³⁵ over the expected 8-ve $[\text{MAu}_{24}(\text{SR})_{18}]^{2-}$ spherical aromatic species, suggests the pronounced reminiscence of aromatic properties in the $[\text{MAu}_{12}]^{6+}$ cores. To evaluate such behavior, we unraveled the characteristics of the induced magnetic field.

Figure 3. Magnetic response properties of the representative



$[\text{PtAu}_{12}]^{6+}$ and $[\text{PtAu}_{12}]^{4+}$ cores. Isosurfaces set to ± 3 ppm, blue means shielding; red - deshielding.

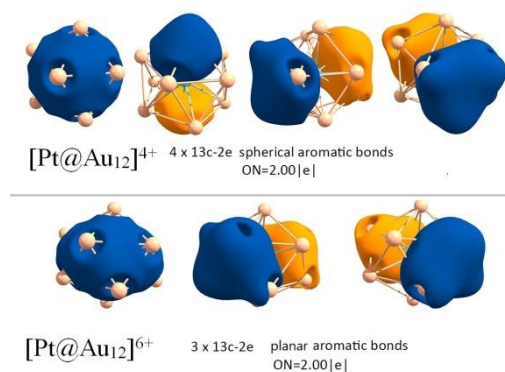


Figure 4. Chemical bonding pattern for $[\text{PtAu}_{12}]^{4+}$ and $[\text{PtAu}_{12}]^{6+}$, as shown by the AdNDP analysis. ON stands for occupation number.

Interestingly, the shielding cone properties observed for spherical aromatic cores are no longer available with the striking exception of the external field oriented perpendicularly to the plane where 1P_x and 1P_y orbitals from the superatomic electronic shells (Figure 3). For other representative directions (along the x- and y-axis), a short-ranged response is found, which after averaging displays both shielding and deshielding regions as can be seen from its $\text{B}_{\text{iso}}^{\text{ind}}$ isosurface, which further confirms the non-spherical aromatic character for 6-ve $[\text{MAu}_{12}]^{6+}$ cores. Moreover, the capability to sustain a shielding cone property upon a parallel oriented field strongly resembles the behavior of par excellence aromatic molecule upon different orientations of the field.^{73,74} Benzene sustains a shielding cone property when the field is parallelly oriented to the molecular plane (along z-axis), denoting a short-ranged response for x- and y-orientations.⁷³ However, we believe that investigated $[\text{MAu}_{12}]^{6+}$ core is an extraordinary case of σ -aromaticity in gold clusters. Aromatic bonds are

constructed from superatomic valence shell $1S^21P_x y^4$ which fully correlates with their shape. The first bond from the set of three 13c-2e has no nodal plane whereas other two have one nodal plane each meaning that they are formed from the parental P orbitals. This contrasts to the canonical π -aromatics like benzene in which all three aromatic bonds have one nodal plane and resemble P orbitals. Noteworthy, that σ -aromaticity was initially proposed for Li and Mg clusters by Alexandrova and Boldyrev,⁷⁵ but recently was experimentally confirmed and shown to exist even in bottled compound $C_6(SePh)_6^{2+}$ by Saito and co-workers.⁷⁶

Thus, our results reveal that the 6-ve $[MAu_{12}]^{6+}$ core from $[MAu_{24}(SR)_{18}]^0$ species, bearing three 13c-2e delocalized bonds, exhibits an unprecedented for quasi-spherical cages planar σ -aromatic behavior. Obviously, it confirms the presence of planar σ -aromatic species in the field of ligand-protected gold clusters. These planar aromatic characteristics support the preferred stability of 6-ve $[MAu_{24}(SR)_{18}]^0$ and the further reversible 6-ve \leftrightarrow 8-ve interconversion. Moreover, it enables controlled shift between planar σ -aromatics and Hirsch's three-dimensional aromatics fulfilling $(4N+2)$ and $2(N+1)^2$ rules, respectively. Therefore, planar σ -aromatic cores can be further manipulated electrochemically in order deliver spherical aromatic species in doped clusters derived from $Au_{25}SR_{18}$ superatom. Overall, superatomic clusters are shown to have inherent and versatile feature to sustain both spherical and planar σ -aromatic characteristics that can be controlled by tuning of their charge states. Moreover, this aromaticity discussion opens intriguing questions of what kind of aromatics is the 18-ve gold core fulfilling both $4N+2$ and $(2N+1)^2$ rules and we aim to enlighten it in our future study.

Conclusions

Here we have revealed and confirmed the inherent spherical aromatic properties of the superatomic 8-electron $Au_{25}(SR)_{18}^-$ clusters ascribed to its inner $[Au_{13}]^{5+}$ core, by the capabilities to sustain a shielding cone property upon different orientations of the applied field, as it is characteristic for Hirsch aromatics. The 8-ve count leads to a set of four 13c-2e delocalized orbitals accounting for the $1S^21P^6$ superatomic electronic shell. Such features also are observed in the Pd and Pt monodoped 8-ve $[MAu_{12}]^{4+}$ cores found in $MAu_{24}(SR)_{18}^{2-}$, supporting the spherical aromatic behavior in other superatomic cores. By contrast, the 6-ve cluster cores from preferred $MAu_{24}(SR)_{18}^0$ species denotes a set of three 13c-2e delocalized orbitals leading to a shielding cone property reserved only for a perpendicularly oriented field about the plane where $1P_x$ and $1P_y$ shells lie, which is an inherent feature for planar aromatics. Thus, the behavior of 6-ve $[MAu_{12}]^{6+}$ cores is the first result showcasing the formation of planar σ -aromatics in quasi-spherical clusters owing to its $1S^21P_x y^4$ superatomic electronic shell.

Conflicts of interest

There are no conflicts to declare.

Acknowledgments

This project was supported by the National Science Foundation (CHE-1664379 to A.I.B.). A.M.-C. thanks financial support from FONDECYT 1180683.

Notes and references

- 1 M. Brust, M. Walker, D. Bethell, D. J. Schiffrin and R. Whyman, *Chem. Commun.*, 1994, 801–802.
- 2 H. Qian, Y. Zhu and R. Jin, *ACS Nano*, 2009, **3**, 3795–3803.
- 3 R. L. Whetten, J. T. Khoury, M. M. Alvarez, S. Murthy, I. Vezmar, Z. L. Wang, P. W. Stephens, C. L. Cleveland, W. D. Luedtke and U. Landman, *Adv. Mater.*, 1996, **8**, 428–433.
- 4 L. A. Oro, P. Braunstein and P. R. Raithby, *Metal clusters in chemistry*, Wiley-vch Weinheim, Germany, 1999, vol. 3.
- 5 M.-C. Daniel and D. Astruc, *Chem. Rev.*, 2004, **104**, 293–346.
- 6 M. W. Heaven, A. Dass, P. S. White, K. M. Holt and R. W. Murray, *J. Am. Chem. Soc.*, 2008, **130**, 3754–3755.
- 7 M. Walter, J. Akola, O. Lopez-Acevedo, P. D. Jadzinsky, G. Calero, C. J. Ackerson, R. L. Whetten, H. Grönbeck, H. Häkkinen, H. Gronbeck and H. Hakkinen, *Proc. Natl. Acad. Sci.*, 2008, **105**, 9157–9162.
- 8 P. Jena, *J. Phys. Chem. Lett.*, 2013, **4**, 1432–1442.
- 9 S. Knoppe, I. Dolamic and T. Bürgi, *J. Am. Chem. Soc.*, 2012, **134**, 13114–13120.
- 10 Y. Levi-Kalisman, P. D. Jadzinsky, N. Kalisman, H. Tsunoyama, T. Tsukuda, D. A. Bushnell and R. D. Kornberg, *J. Am. Chem. Soc.*, 2011, **133**, 2976–2982.
- 11 J. M. Galloway, J. P. Bramble, A. E. Rawlings, G. Burnell, S. D. Evans and S. S. Staniland, *Small*, 2012, **8**, 204–208.
- 12 R. Jin, *Nanoscale*, 2015, **7**, 1549–1565.
- 13 M. Zhu, C. M. Aikens, F. J. Hollander, G. C. Schatz and R. Jin, *J. Am. Chem. Soc.*, 2008, **130**, 5883–5885.
- 14 R. Jin, *Nanoscale*, 2010, **2**, 343–362.
- 15 A. Dass, R. Guo, J. B. Tracy, R. Balasubramanian, A. D. Douglas and R. W. Murray, *Langmuir*, 2008, **24**, 310–315.
- 16 R. Tsunoyama, H. Tsunoyama, P. Pannopard, J. Limtrakul and T. Tsukuda, *J. Phys. Chem. C*, 2010, **114**, 16004–16009.
- 17 H. Häkkinen, *Chem. Soc. Rev.*, 2008, **37**, 1847–59.
- 18 T. Tsukuda, H. Tsunoyama and H. Sakurai, *Chem. Asian J.*, 2011, **6**, 736–748.
- 19 Y. Zhu, H. Qian and R. Jin, *J. Mater. Chem.*, 2011, **21**, 6793–6799.
- 20 K. Kwak, S. S. Kumar and D. Lee, *Nanoscale*, 2012, **4**, 4240–4246.
- 21 N. Sakai and T. Tatsuma, *Adv. Mater.*, 2010, **22**, 3185–3188.
- 22 Z. Wu, M. Wang, J. Yang, X. Zheng, W. Cai, G. Meng, H. Qian, H. Wang and R. Jin, *Small*, 2012, **8**, 2028–2035.
- 23 R. W. Murray, *Chem. Rev.*, 2008, **108**, 2688–2720.
- 24 G. Guan, S.-Y. Zhang, Y. Cai, S. Liu, M. S. Bharathi, M. Low,

- Y. Yu, J. Xie, Y. Zheng, Y.-W. Zhang and M.-Y. Han, *Chem. Commun.*, 2014, **50**, 5703.
- 25 X. Kang, H. Chong and M. Zhu, *Nanoscale*, 2018, **10**, 10758–10834.
- 26 O. Toikkanen, V. Ruiz, G. Rönholm, N. Kalkkinen, P. Liljeroth and B. M. Quinn, *J. Am. Chem. Soc.*, 2008, **130**, 11049–11055.
- 27 H. Qian, C. Liu and R. Jin, *Sci. China Chem.*, 2012, **55**, 2359–2365.
- 28 P. Maity, S. Xie, M. Yamauchi and T. Tsukuda, *Nanoscale*, 2012, **4**, 4027–4037.
- 29 H. Häkkinen, *Nat. Chem.*, 2012, **4**, 443–455.
- 30 S. N. Khanna and P. Jena, *Phys. Rev. B*, 1995, **51**, 13705–13716.
- 31 D. Jiang and S. Dai, *Inorg. Chem.*, 2009, **48**, 2720–2.
- 32 F. K. Sheong, J.-X. Zhang and Z. Lin, *Inorg. Chem.*, 2016, **55**, 11348–11353.
- 33 H. Qian, D. Jiang, G. Li, C. Gayathri, A. Das, R. R. Gil and R. Jin, *J. Am. Chem. Soc.*, 2012, **134**, 16159–16162.
- 34 Y. Niihori, W. Kurashige, M. Matsuzaki and Y. Negishi, *Nanoscale*, 2013, **5**, 508–512.
- 35 K. Kwak, Q. Tang, M. Kim, D. Jiang and D. Lee, *J. Am. Chem. Soc.*, 2015, **137**, 10833–10840.
- 36 Z. Chen, H. Jiao, A. Hirsch and W. Thiel, *J. Mol. Model.*, 2001, **7**, 161–163.
- 37 A. Hirsch, Z. Chen and H. Jiao, *Angew. Chemie Int. Ed.*, 2000, **39**, 3915–3917.
- 38 M. Bühl and A. Hirsch, *Chem. Rev.*, 2001, **101**, 1153–1184.
- 39 J. Aihara, *J. Am. Chem. Soc.*, 1978, **100**, 3339–3342.
- 40 N. Fedik, M. Kulichenko and A. I. Boldyrev, *Chem. Phys.*, 2019, **522**, 134–137.
- 41 C. Liu, N. V. Tkachenko, I. A. Popov, N. Fedik, X. Min, C.-Q. Xu, J. Li, J. E. McGrady, A. I. Boldyrev and Z.-M. Sun, *Angew. Chemie Int. Ed.*, 2019, 1–6.
- 42 A. Muñoz-Castro, *Phys. Chem. Chem. Phys.*, 2017, **19**, 12633–12636.
- 43 A. Muñoz-Castro, *J. Phys. Chem. C*, 2012, **116**, 17197–17203.
- 44 D. Y. Zubarev and A. I. Boldyrev, *J. Phys. Chem. A*, 2009, **113**, 866–868.
- 45 M. Kulichekno, N. Fedik, K. V. Bozhenko, A. I. Boldyrev, *J. Phys. Chem. B*, 2019, **123**, 4065–4069.
- 46 G. Liu, N. Fedik, C. Martinez-Martinez, S. M. Ciborowski, X. Zhang, A. I. Boldyrev, K. H. Bowen, *Angew. Chemie Int. Ed.*, 2019, **58**, 13789–13793.
- 47 M. Kulichekno, N. Fedik, K. V. Bozhenko, *Chem.: Eur. J.*, 2019, **25**, 5311–5315.
- 48 N. V. Tkachenko, D. Steglenko, N. Fedik, N. M. Boldyreva, R. M. Minyaev, V. I. Minkin, A. I. Boldyrev, *Phys. Chem. Chem. Phys.*, 2019, **21**, 19764–19771.
- 49 O. A. Gapurenko, R. M. Minyaev, N. S. Fedik, V. V. Koval, A. I. Boldyrev, V. I. Minkin, *Struct. Chem*, 2019, **30**, 805–814.
- 50 M. Baranac-Stojanović, *RSC Adv.*, 2014, **4**, 308–321.
- 51 S. Klod and E. Kleinpeter, *J. Chem. Soc. Perkin Trans. 2*, 2001, 1893–1898.
- 52 N. D. Charistos, A. G. Papadopoulos and M. P. Sigalas, *J. Phys. Chem. A*, 2014, **118**, 1113–1122.
- T. Heine, C. Corminboeuf and G. Seifert, *Chem. Rev.*, 2005, **105**, 3889–3910.
- R. Islas, T. Heine and G. Merino, *Acc. Chem. Res.*, 2012, **45**, 215–228.
- J. P. Perdew, K. Burke and Y. Wang, *Phys. Rev. B*, 1996, **54**, 16533–16539.
- J. P. Perdew, K. Burke and M. Ernzerhof, *Phys. Rev. Lett.*, 1996, **77**, 3865–3868.
- S. K. Wolff, T. Ziegler, E. van Lenthe, E. J. Baerends, *J. Chem. Phys.*, 1999, **110**, 7689.
- Amsterdam Density Functional (ADF 2016) Code, Vrije Universiteit: Amsterdam, The Netherlands. Available at: <http://www.scm.com>
- Gaussian 16, Revision C.01, M. J. Frisch, G. W. Trucks, H. B. Schlegel, G. E. Scuseria, M. A. Robb, J. R. Cheeseman, G. Scalmani, V. Barone, G. A. Petersson et al, Gaussian, Inc., Wallingford CT, 2016.
- F. Weigand, R. Ahlrichs, *Phys. Chem. Chem. Phys.*, 2005, **7**, 3297–3305.
- M. Gruber, G. Heimel, L. Romaner, J.-L. Brédas and E. Zojer, *Phys. Rev. B*, 2008, **77**, 165411.
- B. Assadollahzadeh and P. Schwerdtfeger, *J. Chem. Phys.*, 2009, **131**.
- L. Xiao, B. Tollberg, X. Hu and L. Wang, *J. Chem. Phys.*, 2006, **124**, 114309.
- M. P. Johansson, I. Warnke, A. Le and F. Furche, *J. Phys. Chem. C*, 2014, **118**, 29370–29377.
- R. Gershoni-Poranne and A. Stanger, *Chem. Soc. Rev.*, 2015, **44**, 6597–6615.
- A. C. Castro, E. Osorio, J. O. C. Jimenez-Halla, E. Matito, W. Tiznado, G. Merino, *J. Chem. Theory Comput.*, 2010, **6**, 2701–2705.
- G. Merino, A. Vela and T. Heine, *Chem. Rev.*, 2005, **105**, 3812–3841.
- T. Ishida, H. Kanno and J. Aihara, *Bull. Chem. Soc. Jpn.*, 2007, **80**, 2145–2148.
- J. A. N. F. Gomes and R. B. Mallion, *Chem. Rev.*, 2001, **101**, 1349–1384.
- A. Muñoz-Castro and R. B. King, *Inorg. Chem.*, 2017, **56**, 15251–15258.
- N. D. Charistos and A. Muñoz-Castro, *J. Phys. Chem. C*, 2018, **122**, 9688–9698.
- A. Muñoz-Castro, *Chem. Commun.*, 2015, **51**, 10287–10290.
- A. G. Papadopoulos, N. D. Charistos and A. Muñoz-Castro, *ChemPhysChem*, 2017, **18**, 1499–1502.
- P. R. von Schleyer and H. Jiao, *Pure Appl. Chem.*, 1996, **68**, 209–218.
- A. N. Alexandrova and A. I. Boldyrev, *J. Phys. Chem. A*, 2003, **107**, 554–560.
- S. Furukawa, M. Fujita, Y. Kanatomi, M. Minoura, M. Hatanaka, K. Morokuma, K. Ishimura and M. Saito, *Commun. Chem.*, 2018, **1**, 60.